Evaluation of effect of deviations in width of cross-section of connected elements

Akbar Ergashov[1*], *Shukhrat* Shojalilov[1], *Rano* Djumaniyazova[1], and *Kamila* Shipilova[2]

[1]Tashkent State Transport University, Tashkent, Uzbekistan
[2]"Tashkent Institute of Irrigation and Agricultural Mechanization Engineers" National Research University, Tashkent, Uzbekistan

Abstract. The tests were carried out in two stages: at the first stage, the height of the fall of the load was assumed to be insignificant, which did not lead to the destruction of the structure, while its deformation was considered in the elastic stage of the work of materials; at the second stage, the height of the fall of the load was selected based on the condition of bringing the structure to destruction, while the work of the structure in the elastic-plastic stage was studied.

1 Introduction

For most of the reinforced concrete structures, the calculation of the transverse force is decisive when assigning cross-section dimensions and transverse reinforcement, which, for example, in the beams of superstructures of bridges and overpasses sometimes amounts to more than 50% of the total rebar consumption per element. A significant proportion (up to 20%) of the reinforcement of such beams can be replaced by effective external reinforcement in the form of high-strength fabric polymer materials made of carbon fiber widely distributed abroad [1-7]. However, the issues of the development of methods for calculating reinforced concrete beams along inclined sections are still not clear enough in many respects. This is primarily due to the fact that the methods used in national and foreign regulatory documents for calculating strength for transverse force are far from perfect in terms of development, accuracy and reliability and are significantly inferior to the methods for calculating strength under the action of bending moments and longitudinal forces [8-13].

2 Methods

In the process of dynamic impact from the side of the structure, there is a reactive rebuff, determined not only by the parameters of the external impact, but also by the dynamic and stiffness characteristics of the system. The nature of the change in the reaction of the system over time is determined by the readings of pressure sensors. The reaction of the system cannot directly characterize the change in external influence due to the influence of inertia forces [3, 4]. Next, the features of elastic and elastoplastic deformation of the

---

*Corresponding author: ergashov@gmail.com

structure under short-term dynamic loading are considered on the example of a plate. At the factory, measurements were made of the actual dimensions of the width of the welded elements of the box section at the level of horizontal sheets and the mismatch of the sizes of the diagonals of the cross-section (rhomboid). The width of the cross sections of 68 elements of the lower belt of the through truss were measured [14-20].

The load is determined based on the readings of the pressure sensor and accelerometer, which measure at one point of the structure.

To construct the theoretical curve of the normal distribution, the dependencies are used:

$$f(b) = \frac{n}{\sigma_b} \cdot \frac{1}{\sqrt{2\pi}} \exp\left(-\frac{u^2}{2}\right) = \frac{n}{\sigma_b} f(u) \qquad (1)$$

$$u = \frac{b_i - b_0}{\sigma_b} \qquad (2)$$

$$m_1 = \frac{nd}{\sum n_i} \qquad (3)$$

$$\sigma_b = \sqrt{m_2 - m_1^2}; \ \overline{\sigma_b} = 0.5\sigma_b \qquad (4)$$

$$m_2 = \frac{nf^2}{\sum n_i} \qquad (5)$$

where, n is total number of width definitions section width; n_i is width of the i-th section; σ_b is mean square deviation; u is normalized deviation; b_i is width of the i-th section; b_0 is the average value of the cross-section; d is the size of the intervals into which the totality of strength determination is divided:

$$f = d + 1 \qquad (6)$$

According to the results of calculations according to Table 1 average section width $b_0 = 339.97 \ mm$; $\sigma_b = 1.351$; $\overline{\sigma}_b = 0.676$.

Fig.1 shows the experimental value of the distribution of the values of the cross-section width and the theoretical distribution curve according to the normal law.
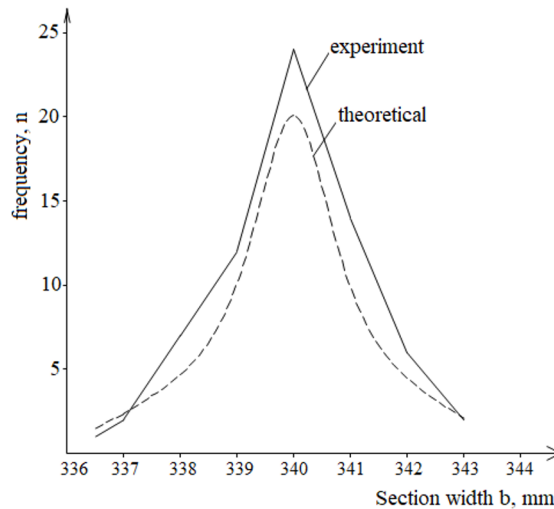

Fig.1. Diagram of the distribution of the actual dimensions of the width of the box section of the lower belt of the truss b, mm

To determine the true law of load change over time, we use the equation of motion of the structure, which in general can be written as follows

$$P_I(t) + P_R(t) = P(t) \qquad (7)$$

where, $P_I(t) = ma(t)$ – inertia forces at a moment of time t; m – the mass of a unit of the plate area, taking into account the weight of the distribution traverse and shield, a bag of water and a falling load; $a(t)$ – accelerations at a moment in time t; $P_R(t)$ – the reaction of the system at a time t; $P(t)$ – actual load at a time t.

The law of load change, calculated by the expression, in the elastic and elastic-plastic stages is shown in fig. 2.

The change in the reaction of the system over time is largely determined by the accelerations of the structure, and, accordingly, the inertia forces depending on them (Fig.2). At the initial stage of loading, accelerations grow intensively simultaneously with the increase in load, while there is no reaction of the system. The inertia forces are directed in the opposite direction with respect to the direction of the load, i.e. at this stage, the inertia forces counteract the external dynamic effect and completely balance it [3, 4].
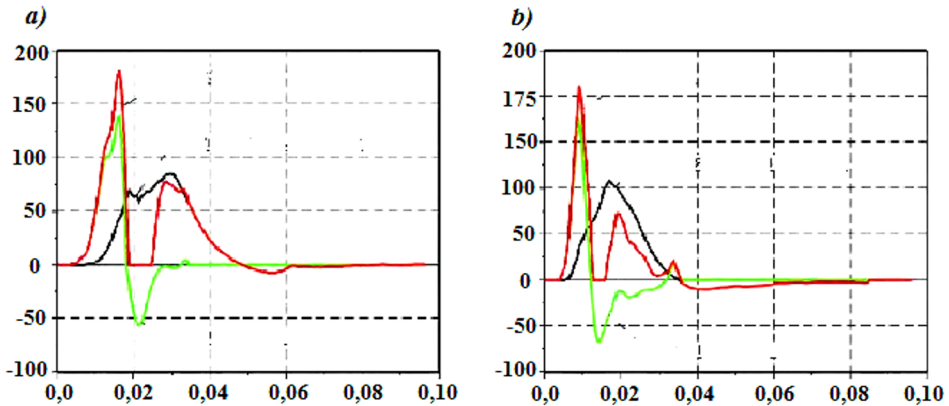

Fig. 2. Distribution of load, reaction of the system and inertia forces over time in the plate in the elastic (a) and elastic-plastic (b) stages of deformation.

Further, as the external load increases, the structure is put into operation, the reaction of the system increases.

The maximum values of the external load and inertia forces are reached simultaneously. When the peak values are reached, the inertia forces make up 76% and 83% of the external load during elastic and elastoplastic deformation of the structure, respectively (Fig. 2).

According to studies, the inertia forces at maximum values can reach 98% of the magnitude of the external dynamic impact. The degree of influence of inertia forces increases with increasing speed of the falling load, creating a dynamic load, at the moment of contact with the structure.

The presented experimental studies also show this trend. When the plate is deformed in the elastic-plastic stage, the effective load is shorter, the load rise time is 5.2 ms, while with elastic deformation it is 13 ms.

After reaching the maximum values, there is almost a one-time decrease in the external dynamic load and inertia forces. When the dynamic load reaches zero, the falling load rebounds, there is no external impact on the structure.

In this case, the plate is under the action of inertia forces only, the direction of which coincides with the direction of the external load. As a result, there is no decrease in the

reaction of the system, its growth either stops and stabilizes at a certain level (Fig.2, a), or growth slows down (Fig.2, b). Repeated impact after rebound leads to an increase in the reaction to the maximum value.

The nature of the resistance of the structure described above can be traced by the readings of all acceleration sensors.

The development of displacements in all the studied points of the structure begins with an increase in the reaction of the system, with a certain lag in relation to the moment of the beginning of the external load, regardless of the stage of operation of the structure. The maximum displacement value is also reached with a lag from the peak of the load and the reaction of the system. In all cases, the lag of movements is due to the influence of inertia forces.

The nature of the distribution of displacements over the plate field at the stage of elastic deformation is uniform, the greatest values of displacements are in the center of the plate. As you move away from the center, the amount of displacement decreases evenly, as a result of moving the plate at the location of the sensors are almost equal.

At the stage of elastic-plastic deformation of the plate, the plate is divided by the joints of plasticity into 4 disks, as a result of which the greatest changes are observed along the line of the plastic joint, and in the areas between the joints the movements are much lower. The deformed plate scheme is close to the pyramidal one.

The change in the deformations of concrete and reinforcement over time also occurs with a lag from the reaction of the system both at the initial stage and when the maximum values are reached. The specified character of the development of deformations takes place both in the elastic and in the elastic-plastic stage of the plate operation.

In the elastic deformation stage of the plate, deformations of compressed concrete and stretched reinforcement reach values of $20 ... 25 \times 10^{-5}$, after which they decrease to values of $6 ... 10 \times 10^{-5}$ and remain at this level.

The decrease is not to zero level due to the static action of the falling load, which remains lying on the structure after impact.

Most of the strain gauges registering concrete tensile deformations fail (break off) at the initial stages of the development of deformations. The readings of the remaining sensors in service show a maximum of 36×10^{-5} deformations.

In the elastic-plastic stage of deformation, the greatest compression deformations occur in the plastic zone. At the same time, compression deformations in the blocks between the joints of plasticity increase at the initial stages (with elastic deformation of the structure), and then, as plastic deformations develop in the reinforcement, they decrease, which indicates the reverse bending of the blocks and the concentration of deformations in the plastic joints.

The maximum compression deformations are $\mathscr{E}_B = 86.7 \times 10^{-5}$, which is below the limit values. The residual deformations of concrete are $\mathscr{E}_B \leq 21.7 \times 10^{-5}$.

The deformations of the reinforcement reach values corresponding to the yield strength, after which they fail. Irreversible plastic deformations of the reinforcement according to the readings of the strain gauges Tr-1 and Tr-3 are $\mathscr{E}_S \leq 60 ... 100 \times 10^{-5}$.

Since the stresses in the reinforcement reach the physical flow limit, and in compressed concrete the stresses are below the limit value, the plate is not over-reinforced, $\xi < \xi_r$.

In the elastic stage of the plate operation, the reference reaction is distributed proportionally in accordance with the design scheme of the plate. In the elastic-plastic stage of the plate operation, the support reaction is redistributed from the supports on the short side of the plate to the supports on the long side.

The proposed theoretical model. In equations for calculating the shear resistance of a special disk model based on analogy with the theory of shear friction are proposed. This theory was briefly discussed in the first chapter and presents a method for estimating the

ultimate shear stresses transmitted through the cracks of a reinforced concrete element.

The concrete surfaces of the crack are rough and irregular and when displacement occurs along the shear plane, its banks will move apart, which will lead to additional tensile stresses in the internal steel reinforcement crossing the crack and compressive stresses in the concrete.

The compressive stress across the crack provides resistance to shear displacement due to friction between the rough surfaces of the crack. It is assumed that the crack opening can lead to the fluidity of the rods crossing the crack. Therefore, the value of tga represents the coefficient of friction between the crack surfaces.

It is also necessary to point out diagrams at high rates of stress changes that are used in the calculations of structures for dynamic impacts (including special ones - shock, explosive and seismic). The resulting loads are characterized by a short duration of action - from a few milliseconds to seconds, as well as suddenness of occurrence. High intensity, short duration, rarity and extremity of the situation determine the peculiarities of approaches to the calculation of structures under such loads. Thus, when an emergency dynamic load is applied, only one requirement is imposed on structures: they must withstand the load without collapsing. Therefore, in most cases, constructions are calculated only for the first group of limit states. For individual structures, deformation is allowed at the stage of destruction, when the load-bearing capacity of the structure decreases due to the gradual destruction of compressed concrete. Therefore, the main feature of the calculation methods for the effect of short-term dynamic loads is the study of the behavior of structures in the plastic stage.

These methods can be divided into three groups: simplified, approximate and accurate. In the first two methods, high-speed loading changes the deformation diagrams of concrete, increasing the values of the elastic modulus, the boundaries of microcracking, and the strength limits. In the simplified method, plastic deformations are concentrated in plastic hinges, turning the structure into a mechanism.

For the development of accurate methods of dynamic calculation of structures, broader information is required, namely:

a) the laws of dynamic deformation of concrete; b) data on the effect of reinforcement on concrete deformations; c) assessment of the stress-strain state of sections of reinforced concrete structures during plastic deformation; d) the laws of adhesion of reinforcement with concrete.

This approach is based on a certain idealization of the properties of reinforced concrete structures, which makes it difficult and sometimes impossible to solve a number of problems. This approach makes it possible to adequately display the processes of deformation of the structure in the entire range of changes in its mechanical properties, which allows us to fully meet the needs of design practice.

3 Conclusion

The presented brief analysis shows that despite certain successes in the development for calculating iron-ton structures, they require further refinement and development. First of all, this concerns the normalization (with 95% security) of the basic parameters of the initial complete diagrams of simple compression and stretching for the main types of structural concrete on the basis of statistically sufficiently representative experimental data. The physical adequacy of such diagrams depends on the completeness of taking into account the main structural and technological factors that determine these parameters. The huge amount and complex nature of the empirical data used in this case do not allow using classical statistical methods for their processing. In our opinion, the most effective methods of processing and using such information are factor analysis based on the principles of

experimental planning and structural simulation modeling of concrete deformation and crack formation processes based on fracture mechanics approaches.

References

1. Ishanxodjaev, A. A., Bekmirzaev, D. A., Ospanov, R. S., Axmedov, S. B., and Usmonov, D. T. Influence of the inertia force of underground pipeline systems under seismic loads. In AIP Conference Proceedings, Vol. 2637, No. 1, p. 050002. (2022).

2. Miralimov, M. Numerical approach for assessment of stress strain state of road culverts. In AIP Conference Proceedings, Vol. 2637, No. 1, p. 050003. (2022).

3. Ahmedov, S. B., Rajabov, T. Y., Shojalilov, S. S., Ergashev, A. T., and Mirzaolimov, I. Y. Multivariate statistical modeling of strength and parameters of diagrams σ b–ε b for expanded clay concrete. In AIP Conference Proceedings, Vol. 2637, No. 1, p. 050005. (2022).

4. Saatova, N., Shozhalilov, S., and Safarov, S. Methodology of techno-economic feasibility study for the reconstruction of road bridges. In AIP Conference Proceedings, Vol. 2432, No. 1, p. 030096. (2022).

5. Axmedov Sh.B. Strength of rc elements strengthened with external fiber polymerreinforcement. International Journal of Advanced Research in Science, Enjineering and technology. Vol. 6(9), 2019).

6. Sh.B.Axmedov., Ashrabov. A. A. On sheer force transfer across the cracks in RC elements. Journal of AN RUz "Problems of mechanics", № 4, pp. 25-29. (2016).

7. Vaghefi, K., Ahlborn, T. T. M., Harris, D. K., and Brooks, C. N. Combined imaging technologies for concrete bridge deck condition assessment. Journal of Performance of Constructed Facilities, 29(4), 04014102. (2015).

8. Mander J. B. Fragility curve development for assessing the seismic vulnerability of highway bridges. Research Progress and, 89. (1999).

9. Wang, N. Reliability-based condition assessment of existing highway bridges. Georgia Institute of Technology. (2010).

10. Broomfield, J. P. Corrosion of steel in concrete: understanding, investigation and repair. Crc Press. (2023).

11. Taerwe, L. Non-metallic (FRP) reinforcement for concrete structures: proceedings of the second international RILEM symposium. CRC Press. (2004).

12. Schaumann, P., and Upmeyer, J. Composite bridges with precast concrete slabs. (1998).

13. Adilov, F. F., Miralimov, M. H., and Abirov, R. A. To the stability of the roadbed reinforced with gabions. In IOP Conference Series: Materials Science and Engineering, Vol. 913, No. 4, p. 042066. (2020).

14. B.A. Khudayarov. Nonlinear flattor of viscoelastic plastic plates, (2013).

15. F.B. Badalov. Dynamic absorbers of vibrations of hereditarily deformable systems", The Uzbek mathematical (2003).

16. Mirsaidov, M. M., and Sultanov, T. Z. Assessment of stress-strain state of earth dams with allowance for non-linear strain of material and large strains. Inzenerno-Stroitel'nyj Zurnal, (5), 73. (2014).

17. Mirsaidov, M. M., Sultanov, T. Z., and Sadullaev, S. A. Determination of the stress-strain state of earth dams with account of elastic-plastic and moist properties of soil and large strains. Inzenerno-Stroitel'nyj Zurnal, (5), 59. (2013).

18. Adilov, F. F., Miralimov, M. H., and Abirov, R. A. To the stability of the roadbed reinforced with gabions. In IOP Conference Series: Materials Science and Engineering, Vol. 913, No. 4, p. 042066. (2020).

19. Rossikhin, Y. A. Reflections on two parallel ways in the progress of fractional calculus in mechanics of solids. Applied Mechanics Reviews, 63(1). (2010).

20. Golub, V. P. Modelling of deformation and fracture processes of structural materials under creep conditions. ZAMM Zeitschrift fur Angewandte Mathematik und Mechanik, 76(Suppl. 5), 169-170. (1996).